

Phenomenology of exotic particles in E_6 theories

Thomas G. Rizzo

Ames Laboratory and Department of Physics, Iowa State University, Ames, Iowa 50011

(Received 14 March 1986)

We explore the properties of the exotic fermions as well as the additional gauge boson(s) and Higgs scalars present in E_6 grand unified theories resulting from superstrings. Special attention has been paid to the decay modes of these new particles and their production mechanisms at existing accelerators and those under construction.

I. INTRODUCTION

The advent of superstring theories¹ (ST's) has revitalized interest in grand unified theories (GUT's) based on the gauge group E_6 (Ref. 2). ST's have the promise of being complete and finite theories of all of the fundamental forces, including gravity. It has been shown³ that such theories are also free of electroweak and gravitational anomalies if the gauge group is either $SO(32)$ or $E_8 \times E_8$ in ten space-time dimensions. It has also been shown that upon compactification down to four dimensions E_8 breaks to E_6 with local $N=1$ supersymmetry (SUSY) below the Planck scale. The second E_8 , unbroken by compactification, is associated with a new form of matter (shadow matter⁴) which only interacts with "normal" matter via gravity. The fermions in E_6 then transform as (at least) three 27 representations with the possibility that "mirror" fermions (Ref. 5) ($\bar{27}$) may also be present. Investigations^{6,7} have also shown that at low energies ($\lesssim 1-10$ TeV) the effective electroweak gauge group resulting from E_6 breaking is larger than that in the standard model (SM) by (at least) an additional $U(1)$ factor. Additional sets of Higgs bosons will inevitably be necessary to break this $U(1)$ and produce masses for all the various fermions.

It is thus quite clear that the simplest extension of the SM suggested by ST's (via E_6) contains new exotic fermions (twelve per generation), an additional gauge boson associated with the new $U(1)$ factor, plus an extension of the SM scalar sector beyond a single isodoublet (or two isodoublets in SUSY versions). The purpose of this paper is to begin an exploration of some of the new phenomenology resulting from such a large extension of the SM. Our work is far from complete but it is an important step to take if we are to test, even indirectly, the predictions of ST.

The paper is organized as follows. Section II contains a general discussion of the particle content of the low-energy effective theory as a result of E_6 breaking as well as particle mixing. The general form of the charged- and neutral-current couplings of all the particles are discussed. The flavor-changing neutral-current couplings are also given. Section III deals with the decay properties of the new charged fermions in the model. These various decay modes are quite sensitive to the mass spectrum in the theory. In Sec. IV we discuss various mechanisms for producing these new fermions at existing accelerator and

those currently under construction. Section V contains a brief discussion of some of the new physics associated with the extended Higgs sector of this new class of models. Our results and our conclusions can be found in Sec. VI.

II. EFFECTIVE LOW-ENERGY THEORY

A. General discussion

The fermion content of a single E_6 27 representation is given by

$$\begin{aligned} & \begin{pmatrix} \nu \\ e \end{pmatrix}_L, \begin{pmatrix} u \\ d \end{pmatrix}_L, e_R, u_R, d_R, \nu_R, \\ & \begin{pmatrix} N \\ E \end{pmatrix}_L, \begin{pmatrix} N' \\ E \end{pmatrix}_R, D_L, D_R, \nu'_L. \end{aligned} \tag{2.1}$$

The second row consists of the eleven new "exotic" fermions which appear in the 27 but not in the 16 of $SO(10)$. In addition to their obvious $SU(2)_L \times U(1)_Y$ quantum numbers, the breaking of E_6 leads to an additional $U(1)_X$ local gauge symmetry at low ($\approx 1-10$ TeV) energies as mentioned above. The electric charge Q and the $U(1)_X$ generator T_x are orthogonal so that $Q = T_3 + Y/2$ as in the SM. Note $Q(N, N', \nu') = 0$, $Q(E) = -1$, and $Q(D) = -\frac{1}{3}$. This implies that the $SU(3)_C \times U(1)_{EM}$ quantum numbers (as well as lepton and baryon numbers) of the fields e and E (d and D) are identical so that mixing can occur between these fields. This has been a subject of much discussion in the literature.⁸ Similar (but more complex) mixings can also occur between the neutral fields ν_L, ν_R, N_L, N_R , and ν'_L . This mixing will play a very important role in the decay and production properties of the exotic fermions.

Table I shows a list of the $U(1)_X$ quantum numbers of all the members of the $\bar{27}$ representation for four different possible $U(1)_X$'s resulting from E_6 breaking. These breaking patterns have been discussed in detail in our previous work⁷ so we will merely summarize the origins of the various $U(1)_X$'s below:

$$\begin{aligned}
\text{A: } E_6 &\rightarrow \text{SO}(10) \times \text{U}(1)_X \rightarrow \text{SU}(5) \times \text{U}(1)_X \rightarrow 3_C 2_L 1_Y 1_X, \\
\text{B: } E_6 &\rightarrow \text{SO}(10) \rightarrow \text{SU}(5) \times \text{U}(1)_X \rightarrow 3_C 2_L 1_Y 1_X, \\
\text{C: } E_6 &\rightarrow \text{SU}(6) \times \text{SU}(2) \rightarrow \text{SU}(6) \rightarrow \text{SU}(5) \times \text{U}(1)_X \\
&\rightarrow 3_C 2_L 1_Y 1_X, \\
\text{D: } E_6 &\rightarrow \text{SU}(6) \times \text{SU}(2) \rightarrow \text{SU}(6) \times \text{U}(1)_X \\
&\rightarrow \text{SU}(5) \times \text{U}(1)_X \rightarrow 3_C 2_L 1_Y 1_X.
\end{aligned} \tag{2.2}$$

Note that pattern (C) has attracted the most attention in the literature.

Let us now turn to a simplified treatment of the mixings between the fermions discussed above. Defining the weak-eigenstate fields to be $e^0, E^0 (d^0, D^0)$, etc., the physical fields are obtainable by a unitary transformation. Let

$$\mathcal{E}_{L,R}^0 \equiv \begin{pmatrix} e^0 \\ E^0 \end{pmatrix}_{L,R}, \quad \mathcal{D}_{L,R}^0 \equiv \begin{pmatrix} d^0 \\ D^0 \end{pmatrix}_{L,R} \tag{2.3}$$

then the unphysical fields are given by

$$\mathcal{E}_{L,R} = U_{L,R}(e) \mathcal{E}_{L,R}^0, \quad \mathcal{D}_{L,R} = U_{L,R}(d) \mathcal{D}_{L,R}^0, \tag{2.4}$$

where, for simplicity, we take the matrices U to be real and orthogonal:

$$U_{L,R}(e) = \begin{pmatrix} \cos\theta_{L,R}^e & \sin\theta_{L,R}^e \\ -\sin\theta_{L,R}^e & \cos\theta_{L,R}^e \end{pmatrix}, \text{ etc.} \tag{2.5}$$

As has been noted,⁸ these mixings produce flavor-changing neutral currents (FCNC's) since the Glashow-Weinberg-Paschos⁹ conditions are not satisfied. These FCNC's may be critical in understanding the decay modes of the new fermions. We note further that the matrices U_L and U_R are, in general, distinct since fermion-mass matrices are not always Hermitian. This will be discussed

later in our analysis below. We now turn to a discussion of the various couplings of these fermions.

B. Interactions

The neutral-current interactions for any fermion f in the weak-eigenstate basis is described by the Lagrangian

$$\begin{aligned}
L_{\text{NC}} = & \frac{g}{2c_W} \bar{f} \gamma_\mu [(T_{3L} + T_{3R} - 2x_W Q) \\
& - (T_{3L} - T_{3R}) \gamma_5] f Z_1^\mu \\
& + \frac{g_x}{2} \bar{f} \gamma_\mu [(X_L + X_R) - (X_L - X_R) \gamma_5] f Z_2^\mu. \tag{2.6}
\end{aligned}$$

In writing down this expression we have neglected any mixing between the two neutral gauge bosons $Z_{1,2}$ (this mixing has been shown to be quite small in our earlier work¹⁰). $X_{L(R)}$ is the value of the $\text{U}(1)_X$ generator T_X for $f_{L(R)}$ which can be read off from Table I and $x_W \equiv \sin^2\theta_W \simeq 0.217$. Also, Q is the fermion charge, T_{3L} (T_{3R}) is the value of the third component of weak isospin for $f_{L(R)}$, and g_X is the $\text{U}(1)_X$ coupling constant.

Once we allow for fermion mixing the Lagrangian in the mass-eigenstate basis can be written as

$$\begin{aligned}
L_{\text{NC}} = & \frac{g}{2c_W} \sum_{\alpha,\beta} \bar{f}_\alpha \gamma_\mu (v_1 - a_1 \gamma_5) f_\beta Z_1^\mu \\
& + \frac{g_x}{2} \sum_{\alpha,\beta} \bar{f}_\alpha \gamma_\mu (v_2 - a_2 \gamma_5) f_\beta Z_2^\mu. \tag{2.6'}
\end{aligned}$$

Tables II and III show the values of v_i and a_i for the physical fields e, E, d , and D in terms of the mixings described earlier in the previous section. Note the pres-

TABLE I. Values of the $\text{U}(1)_X$ quantum numbers for the various fermions in the 27 representation of E_6 in models A–D.

	A		B		C		D	
	X_L	X_R	X_L	X_R	X_L	X_R	X_L	X_R
ν_L	1	0	3	0	-1	0	$\frac{1}{2}$	0
e_L	1	0	3	0	-1	0	$\frac{1}{2}$	0
d_R	0	-1	0	-3	0	1	0	$-\frac{1}{2}$
u_R	0	-1	0	1	0	-2	0	0
e_R	0	-1	0	1	0	-2	0	0
u_L	1	0	-1	0	2	0	0	0
d_L	1	0	-1	0	2	0	0	0
ν_R	0	-1	0	5	0	-5	0	$\frac{1}{2}$
N_L	-2	0	-2	0	-1	0	$-\frac{1}{2}$	0
E_L	-2	0	-2	0	-1	0	$-\frac{1}{2}$	0
D_R	0	2	0	2	0	1	0	$\frac{1}{2}$
N_R	0	2	0	-2	0	4	0	0
E_R	0	2	0	-2	0	4	0	0
D_L	-2	0	2	0	-4	0	0	0
ν'_L	4	0	0	0	5	0	$\frac{1}{2}$	0

TABLE II. Values of the vector and axial-vector couplings of the (e, E) and (d, D) fermions to the Z_1 .

α	β	v_1	a_1
e	e	$-\frac{1}{2} + 2x_W - \frac{1}{2}(s_R^e)^2$	$-\frac{1}{2}(c_R^e)^2$
E	E	$-\frac{1}{2} + 2x_W - \frac{1}{2}(c_R^e)^2$	$-\frac{1}{2}(s_R^e)^2$
e	E	$+\frac{1}{2}s_R^e c_R^e$	$-\frac{1}{2}s_R^e c_R^e$
E	e	$+\frac{1}{2}s_R^e c_R^e$	$-\frac{1}{2}s_R^e c_R^e$
d	d	$-\frac{1}{2}(c_L^d)^2 + \frac{2}{3}x_W$	$-\frac{1}{2}(c_L^d)^2$
D	D	$-\frac{1}{2}(s_L^d)^2 + \frac{2}{3}x_W$	$-\frac{1}{2}(s_L^d)^2$
d	D	$-\frac{1}{2}s_L^d c_L^d$	$-\frac{1}{2}s_L^d c_L^d$
D	d	$-\frac{1}{2}s_L^d c_L^d$	$-\frac{1}{2}s_L^d c_L^d$

TABLE III. Same as Table I but for Z_2 .

α	β	v_2/a_2
e	e	$[X_L^e(c_L^e)^2 + X_L^E(s_L^e)^2] \pm [X_R^e(c_R^e)^2 + X_R^E(s_R^e)^2]$
E	E	$[X_L^E(c_L^e)^2 + X_L^E(s_L^e)^2] \pm [X_R^E(c_R^e)^2 + X_R^E(s_R^e)^2]$
e	E	$(X_L^e - X_L^E)s_L^e c_L^e \pm (X_R^e - X_R^E)s_R^e c_R^e$
E	e	$(X_L^e - X_L^E)s_L^e c_L^e \pm (X_R^e - X_R^E)s_R^e c_R^e$
d	d	$[X_L^d(c_L^d)^2 + X_L^D(s_L^d)^2] \pm [X_R^d(c_R^d)^2 + X_R^D(s_R^d)^2]$
D	D	$[X_L^D(c_L^d)^2 + X_L^D(s_L^d)^2] \pm [X_R^D(c_R^d)^2 + X_R^D(s_R^d)^2]$
d	D	$(X_L^d - X_L^D)s_L^d c_L^d \pm (X_R^d - X_R^D)s_R^d c_R^d$
D	d	$(X_L^d - X_L^D)s_L^d c_L^d \pm (X_R^d - X_R^D)s_R^d c_R^d$

ence of nonchiral FCNC's which have important implications to process such as $\mu \rightarrow e\gamma$ and the $g - 2$ of leptons.⁸

We now turn to charged currents; we limit ourselves to a simplified mixing between the neutral fields of the form

$$\eta_{L,R} \equiv U_{L,R}(\nu)\eta_{L,R}^0, \quad \eta_{L,R}^0 = \begin{pmatrix} \nu^0 \\ N^0 \end{pmatrix}_{L,R} \quad (2.7)$$

with the ν_L' field unmixed. The reason for this choice is due to the fact that ν_L' is an SO(10)-singlet field with a null value of $B - L$. ν and N , however, do have the same lepton number and can mix even in the limit of exact lepton-number conservation. We thus obtained the charged-current (CC) interaction for a single generation of the form

$$\begin{aligned} L_{CC} = & \frac{g}{2\sqrt{2}} [\bar{\nu}\gamma_\mu(1-\gamma_5)e + \bar{N}\gamma_\mu(1-\gamma_5)E] \cos(\theta_L^e - \theta_L^\nu) W^\mu + \frac{g}{2\sqrt{2}} [\bar{\nu}\gamma_\mu(1-\gamma_5)E + \bar{N}\gamma_\mu(1-\gamma_5)e] \sin(\theta_L^e - \theta_L^\nu) W^\mu \\ & + \frac{g}{2\sqrt{2}} [\bar{N}'\gamma_\mu(1+\gamma_5)E \cos\theta_R^\nu \cos\theta_R^e + \bar{N}'\gamma_\mu(1+\gamma_5)e \cos\theta_R^\nu \sin\theta_R^e \\ & + \bar{\nu}_R\gamma_\mu(1+\gamma_5)E \cos\theta_R^e \sin\theta_R^\nu + \bar{\nu}_R\gamma_\mu(1+\gamma_5)e \sin\theta_R^\nu \sin\theta_R^e] \\ & + \frac{g}{2\sqrt{2}} \bar{u}\gamma_\mu(1-\gamma_5)(d \cos\theta_L^d + D \sin\theta_L^d) W^\mu + \text{H.c.} \end{aligned} \quad (2.8)$$

As we have noted, in writing down these Lagrangians we have ignored the effects of further generations; the leptonic parts can be easily generalized and in the hadronic terms we need to incorporate Kobayashi-Maskawa¹¹ (KM) mixing to incorporate further generations.

From neutral-current experiments at low energy and e^+e^- data we can conclude that θ_R^e and θ_L^d must be quite small.⁸ Universality of the charged-current interactions constrains θ_L^d and the difference $\theta_L^e - \theta_L^\nu$ also to be quite small. For practical purposes we will assume that $\sin^2\theta$ (where $\theta = \theta_R^e, \theta_L^d$, or $\theta_L^e - \theta_L^\nu$) $\lesssim 0.05$ in our calculations below. Clearly the angles θ_L^ν and θ_L^e are not separately constrained to be small. In addition, note that there are now clear constraints on the angles, θ_R^ν and θ_R^d which may, *a priori*, be quite large. Thus the magnitude of the size of these angles may play a very important role in determining the detailed properties of the new particle.

III. DECAYS OF EXOTIC FERMIONS

The specific decay patterns of the exotic E_6 fermions are quite sensitive to their masses and the various mixing angles discussed above. This can be clearly seen by considering first the case of the D -type quark.

A. D decay modes

In the absence of mixing this particle is an SU(2) singlet with a diagonal neutral current which is a pure vector. Since it does not couple to the W in this limit and FCNC's are absent the D quark is absolutely stable. Clearly the existence of a very heavy ($\gtrsim 23$ GeV from the present DESY PETRA data) stable, charged, strongly interacting particle can be ruled out by cosmology.¹² The only place such a particle could be produced today is at the CERN collider. (Data from the collider may already rule out exotic masses in the range up to ~ 50 GeV.) Thus mixing needs to be introduced between the d and D quarks to ensure compliance with present limits. This mixing allows the D to decay via charged-current or FCNC interactions.

Next, we must ask what the mass of the D is relative to for the various gauge bosons. There are four possible scenarios:

- (I) $M_D < M_W, M_{1,2}$,
- (II) $M_W < M_D < M_1, M_2$,
- (III) $M_W, M_1 < M_D < M_2$,
- (IV) $M_W < M_{1,2} < M_D$,

(3.1)

$M_{1,2}$ are the masses of Z_1 and Z_2 , respectively.

In scenario I, the typical decay modes of the D (with only a single mixing-angle suppression factor) are via virtual gauge bosons

$$\begin{aligned} D &\rightarrow u + W_{\text{virt}}^- \\ &\quad \downarrow \\ &\quad \bar{\nu}e^-, \bar{u}d, \bar{c}s, \text{ etc.}, \\ D &\rightarrow d + (Z_1, Z_2)_{\text{virt}} \\ &\quad \downarrow \\ &\quad e^+e^-, \bar{\nu}\nu, \bar{u}u, \bar{d}d, \text{ etc.} \end{aligned} \quad (3.2)$$

Note that in the case of decay via FCNC's both the Z_1 and Z_2 bosons can contribute to the decay process. Figure 1 shows a generic decay of the D quark of this type ($D \rightarrow \chi ab\bar{c}$) via a generic gauge boson X with a matrix element of the form (the sum extends over the possible intermediate gauge bosons)

$$\begin{aligned} M &= \sum_i \bar{a}(P_2) \gamma_\mu (v_i - a_i \gamma_5) D(P_1) \frac{-g^{\mu\nu} + q^\mu q^\nu / M_i^2}{(q^2 - M_i^2) - i\Gamma_i M_i} \\ &\quad \times \bar{b}(P_3) \gamma_\nu (v'_i - a'_i \gamma_5) c(P_4) \end{aligned} \quad (3.3)$$

with an obvious notation. Since $M_D < M_W, M_{1,2}$ one may examine the limit $M_D^2 \ll M_W^2 M_{1,2}^2$ for which we obtain

$$\begin{aligned} \Gamma(D \rightarrow ab\bar{c}) &= N_c \frac{M_D^5}{384\pi^3} \\ &\quad \times \sum_{i,j} \frac{(v_i v_j + a_i a_j)(v'_i v'_j + a'_i a'_j)}{M_i^2 M_j^2} \end{aligned} \quad (3.4)$$

with N_c the number of colors of the $b\bar{c}$ pairs. If, however, the D is sufficiently heavy such that M_D is less than but still comparable to the mass of a gauge boson (as would the t quark and the W if $m_t \simeq 40$ GeV) then we obtain a more complicated expression:

$$\Gamma(D \rightarrow ue^- \bar{\nu}_e) = \frac{G_F^2 M_D^5}{192\pi^2} (s_L^d)^2 \int_0^{1/2} x^2 dx \frac{48 - 64x}{[\lambda(1-2x) - 1]^2 + \Gamma W^2 / M_W^2} \quad (3.7)$$

with $\lambda \equiv M_D^2 / M_W^2$. The naive expectation (from just scaling μ decay) is of course given by Γ_0 ;

$$\Gamma_0 = \frac{G_F^2 M_D^5}{192\pi^3} (s_L^d)^2, \quad (3.8)$$

and the integral results in an additional enhancement of this decay which is $\simeq 20\%$ for $M_D = 50$ GeV and 80% for $M_D = 70$ GeV.

Similar approximations can be made in the neutral-current channel; with $M_D^2 \ll M_1^2 \ll M_2^2$ we obtain, for example, the decay rate for the process $D \rightarrow de^+e^-$ to be

$$\Gamma(D \rightarrow de^+e^-) = \frac{G_F^2 M_D^5}{192\pi^3} (s_L^d c_L^d)^2 (1 - 4x_W + 8x_W^2) \quad (3.9)$$

which is roughly half of Γ_0 in magnitude. Clearly the W

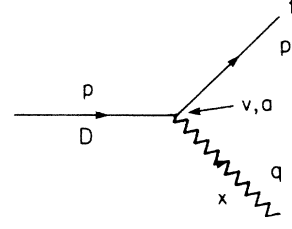


FIG. 1. Feynman diagram for D -quark decay via virtual- X -boson exchange.

$$\begin{aligned} \Gamma(D \rightarrow ab\bar{c}) &= N_c \frac{M_D^5}{48\pi^3} \int_0^{1/2} x^2 dx \sum_{ij} A_{ij} [B_{ij}(9 - 16x) \\ &\quad + C_{ij}(-3 + 8x)], \end{aligned} \quad (3.5)$$

where $x = E_a / M_D$ and where

$$\begin{aligned} A_{ij} &\equiv \frac{(q^2 - M_i^2)(q^2 - M_j^2) + (\Gamma_i M_i)(\Gamma_j M_j)}{[(q^2 - M_i^2)^2 + (\Gamma_i M_i)^2][(q^2 - M_j^2)^2 + (\Gamma_j M_j)^2]}, \\ B_{ij} &\equiv (v_i v_j + a_i a_j)(v'_i v'_j + a'_i a'_j), \end{aligned} \quad (3.6)$$

$$C_{ij} \equiv (v_i a_j + v_j a_i)(v'_i a'_j + v'_j a'_i),$$

with $q^2 = M_D^2(1 - 2x)$. To make use of the full expression, one must know the detailed masses and widths of all the gauge bosons (including Z_2 for which only mass bounds are presently obtainable^{6,7}).

For decay by virtual W the situation simplifies considerably to a much more compact result, for example,

and $Z_{1,2}$ contributions are quite comparable [note $(s_L^2 c_L^d)^2 \simeq (s_L^d)^2$ in the limit of small θ_L^d , which is what is expected]. This can be clearly seen from Table IV which shows D decay branching ratios; in this same case the total lifetime is $21.5\Gamma_0$. We neglect all nonleptonic enhance-

TABLE IV. Branching ratios of the D in the limit $M_D \ll M_W$.

Mode	Branching ratio (%)
$de^- \bar{\nu}_e, d\mu^- \bar{\nu}_\mu, d\tau^- \bar{\nu}_\tau$	4.7
$d\bar{u}d$	7.0
$d\bar{c}s$	14.0
$u\bar{\nu}_1\nu_1, u\bar{\nu}_2\nu_2, u\bar{\nu}_3\nu_3$	4.7
$ue^+e^-, u\mu^+\mu^-, u\tau^+\tau^-$	2.4
$u\bar{u}u$	4.1
$u\bar{c}c$	8.3
$u\bar{d}d, u\bar{s}s, u\bar{b}b$	10.5

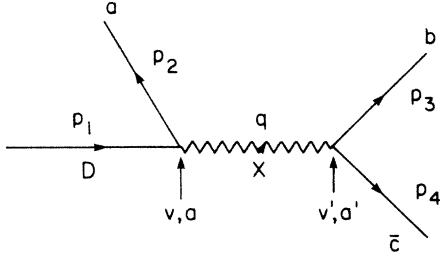


FIG. 2. Same as Fig. 1 but for D decay into a real X boson.

ment effects as well as radiative corrections in these estimates and set KM angles to zero. We also assume that modes involving t quarks do not contribute due to phase-space or kinematical factors and that all other possible decay modes are suppressed. Clearly FCNC effects will be visible in D particle decay.

Once M_D exceeds a gauge boson mass threshold, the D will decay via a two-body process (as shown in Fig. 2) via the matrix element (for $D \rightarrow fX$)

$$M = \bar{D}(p)\gamma_\mu(v - a\gamma_5)f(p')\epsilon_X^\mu \quad (3.10)$$

with a decay rate given by

$$\Gamma(D \rightarrow fX) = \frac{M_D}{16\pi}(v^2 + a^2)\frac{1}{Z^2}(1 - 3Z^4 + 2Z^6) \quad (3.11)$$

with $Z \equiv M_X/M_D$. The three-body decay is suppressed by large numerical factors ($192\pi^3$) as well as an additional factor of g^2 in comparison to the two-body decay. Thus for M_D exceeding M_X the two-body decay clearly dominates. Clearly in scenario II where $M_W < M_D < M_{1,2}$ the decay $D \rightarrow uW^-$ will far and away dominate over the FCNC modes. A plot of the function

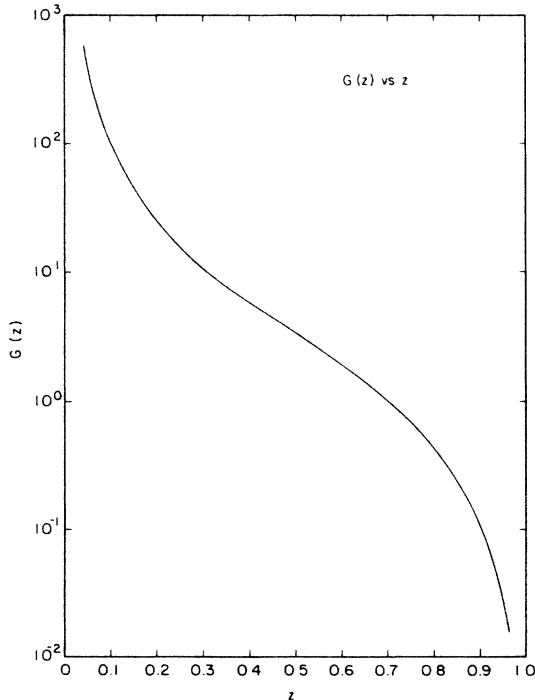


FIG. 3. G as a function of z defined by Eq. (3.11).

$$G(Z) = Z^{-2}(1 - 3Z^4 + 2Z^6)$$

can be found in Fig. 3; note $G \simeq 1$ for $M_X/M_D \simeq 0.7$. In the case of $X = W$ (scenario II),

$$v^2 + a^2 \rightarrow \pi\alpha(s_L^d)^2/x_W,$$

whereas in the case $X = Z_1$ (as can occur in scenario III)

$$v^2 + a^2 \rightarrow \pi\alpha[(s_L^d c_L^d)^2/2x_W(1 - x_W)]$$

that both types of decay have comparable couplings. The Z_1 final state is, however, slightly suppressed by the additional $[2(1 - x_W)]^{-1} \simeq 0.64$ factor. The function G then provides a further suppression of the Z_1 mode (in scenarios III and IV) due to phase space.

Thus in scenario II the $D \rightarrow W^-u$ dominates over all others while in scenario III both $D \rightarrow W^-u$ and $D \rightarrow Z_1d$ are comparable with the W mode being somewhat larger. Clearly this same situation occurs in scenario IV if M_D is not much larger than M_2 . Since the couplings to the Z_2 boson which are flavor changing for the D are small in all models (and g_X^2 itself is small⁷) the two modes $D \rightarrow W^-u$ and $D \rightarrow Z_1d$ remain the most important in scenario IV, i.e., the decay $D \rightarrow Z_2d$ is suppressed relative to both the W^-u and Z_1d modes.

Another, potentially important, decay mode of the D is via single gluon emission ($D \rightarrow dg$) which can proceed through the one-loop diagrams shown in Fig. 4. These diagrams clearly show that there are several different contributions to this process—those from gauge bosons and those from Higgs scalars. As we will see below (and as is alluded to in our earlier work) the Higgs sector contains at least a single (pair) isodoublet and isosinglet in order to generate all the gauge boson and fermion masses. This yields at least two neutral physical Higgs scalars with flavor-changing couplings which can contribute to this one-loop-order process.

An estimate of the decay rate for this process is

$$\Gamma(D \rightarrow dg) = \frac{M_D}{96\pi^2}\alpha^2\alpha_s(\text{mixing angles}) \times F(M_D, M_W, M_{1,2}, M_H). \quad (3.12)$$

F represents a complicated function of the various masses and coupling constants resulting from the diagram and by “mixing angles” we mean those relevant to this flavor-changing process—combinations of $\theta_{L,R}^d$. If F is of order unity, then the usual weak decay modes are at least as large as the gluon-emission process for $M_D > 23$ GeV. As M_D increases, however, the weak decay rate grows quite rapidly. If $M_D > M_W$ the weak two-body decay rate is huge in comparison to the $d + g$ mode even if F is quite large. Clearly, a complete analysis of this process is necessary.

Other unusual decay modes are possible if D is sufficiently heavy. One such possibility of D decay via Higgs-boson emission. As mentioned earlier, the minimal $SU(2)_L \times U(1)_Y \times U(1)_X$ model contains at least two physical Higgs scalars which will have an off-diagonal coupling to $\bar{D}d$. In SUSY versions of this model, a doubling of the number of Higgs multiplets results in charged as well as

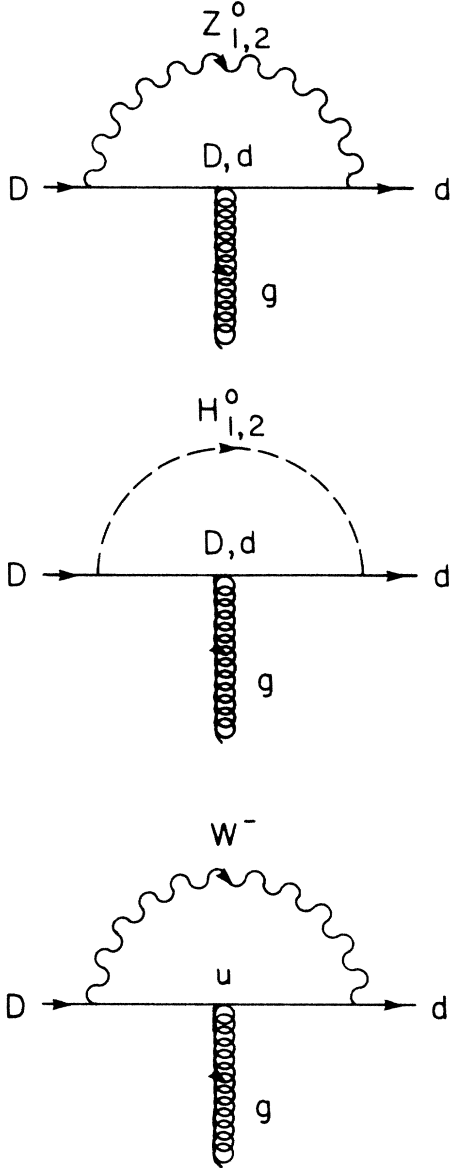


FIG. 4. One-loop diagrams which can contribute to the decay $D \rightarrow dg$.

neutral Higgs fields which could contribute to D decay. A representative graph for this process is shown in Fig. 5(a) and we can take the matrix element for this process to be

$$M = (\sqrt{2}G_F)^{1/2} M_D s_L^d C \bar{u}(p) u(p'), \quad (3.13)$$

where C contains the details of the vertex and is sensitive to the exact structure of the model. C will depend on such factors as (i) the set of vacuum expectation values in the theory, (ii) the mixing among the Higgs fields, (iii) the mixing in the D - d matrix, and (iv) possible KM-type mixing for the $D \rightarrow H^- u$ decay. The decay rate for this process is given by

$$\Gamma = \frac{\sqrt{2}G_F M_D^3}{16\pi} C^2 (1 - M_H^2/M_D^2)^2 (s_L^d)^2 \quad (3.14)$$

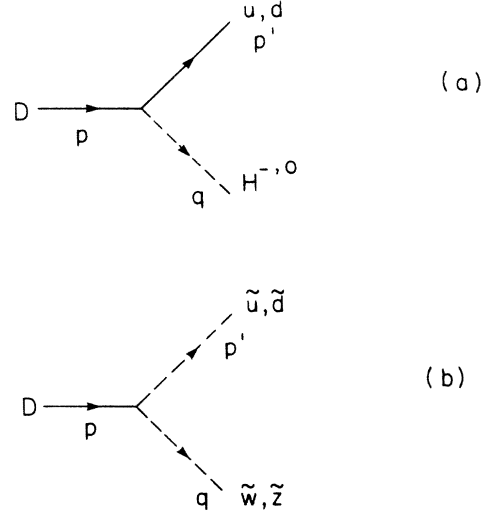


FIG. 5. Some Higgs-boson and supersymmetric decay modes of the D quark.

and so with $C \sim 1$ this process could compete with decay via gauge bosons.

The D may also decay into SUSY final states if the mass of the \tilde{u} and \tilde{d} scalar quarks plus the corresponding gauginos are less than M_D . The relevant diagram for processes such as this is given in Fig. 5(b). Since charged currents couple in a left-handed manner and only the states d_L - D_L mix in a flavor-changing way (since both d_R and D_R are singlets), only the decays $D \rightarrow \tilde{d}_L \tilde{Z}$ and $D \rightarrow \tilde{u}_L \tilde{W}$ are possible. We find the decay rate for this process to be of the form

$$\begin{aligned} \Gamma(D \rightarrow \tilde{f}_L \tilde{X}) &= \frac{M_D \alpha}{32} \left[1 + \left[\frac{m_X^2 - m_f^2}{m_D^2} \right] \right] \\ &\times \left[\left[\frac{m_X^2}{m_D^2} + \frac{m_f^2}{m_D^2} \right]^2 - 4 \frac{m_f^2}{m_D^2} \right]^{1/2} k \end{aligned} \quad (3.15)$$

with

$$\begin{aligned} k(\tilde{W} \tilde{u}_L) &= (4/x_W)(s_L^d)^2, \\ k(\tilde{Z} \tilde{d}_L) &= \left[\frac{2(1-2x_W/3)^2}{x_W(1-x_W)} \right] (s_L^d)^2. \end{aligned} \quad (3.16)$$

Since the k factors, apart from $(s_L^d)^2$, are numerically large, these SUSY decay modes can clearly compete with the usual two-body decay modes unless there is substantial phase space suppression. Similar Higgs-fermion decays are, of course, also possible.

B. E decay modes

The decay modes of the E are somewhat similar to those of the D but with some further modes possible depending on the details of the mass spectrum. This is easily seen by examining the charged-current Lagrangian in Eq. (2.8). If the mass of E is larger than that of N (or N' if N and N' are distinct fields) then E will decay via

charged currents [$E \rightarrow N(N') + W^-$] even in the limit of zero mixing. Clearly this will be the dominant decay mode.

If $M_E - M_N < M_W$ as well then the W boson is virtual as in the decay $E \rightarrow N(N')e^- \bar{\nu}_e$ shown in Fig. 6(a). The decay rate for this process is given by the expression

$$\Gamma(E \rightarrow Ne^- \bar{\nu}_e) = \frac{G_F^2 M_E^5}{12\pi^3} W^2 \int_{\delta}^{(1/2)(1+\delta^2)} dx \frac{(x^2 - \delta^2)^{1/2} [x(1 + \delta^2 - 2x) + 2(1-x)(x - \delta^2)]}{(1 + \delta^2 - 2x - W)^2 + WG}, \quad (3.17)$$

where $W \equiv M_W^2/M_E^2$, $\delta = M_N/M_E$, $G = (\Gamma_W/M_E)^2$, and $x = E_N/M_E$. An identical expression obtains for the decay $E \rightarrow N'e^- \bar{\nu}_e$. If N and N' are identical, then we simply rescale Eq. (3.17) by $(v^2 + a^2)/2$ where $v(a)$ is the appropriately scaled vector (axial-vector) coupling constant at the $\bar{E}NW$ vertex. Simple counting arguments can then be used to estimate various branching ratios for E -decay final states. For example, we estimate

$$\Gamma(E \rightarrow N(N')e^- \bar{\nu}_e) / \Gamma(E \rightarrow \text{all}) \simeq \frac{1}{9} \text{ if } m_t > m_E$$

or if t final states are suppressed.

If $M_E - M_N > M_W$ two-body decay becomes possible [Fig. 6(a)]. For general vector (v) and axial-vector (a) couplings, the $E \rightarrow WN(N')$ decay rate is

$$\begin{aligned} \Gamma(E \rightarrow N, N' W^-) = & \frac{g^2 M_E}{128\pi} \left[\left[1 + \frac{m_N^2 - m_W^2}{m_E^2} \right]^2 - \frac{4m_N^2}{m_E^2} \right]^{1/2} \\ & \times \left[(v^2 + a^2) \left\{ \left[1 + \frac{m_N^2 - m_W^2}{m_E^2} \right] + \frac{m_E^2}{m_W^2} \left[\left[1 - \frac{m_N^2}{m_E^2} \right]^2 - \left[\frac{m_W^2}{m_E^2} \right]^2 \right] \right\} - 6 \frac{m_N}{m_E} (v^2 - a^2) \right]. \end{aligned} \quad (3.18)$$

Note that if N and N' are identical v and a are given by the expressions

$$\left. \begin{array}{l} v \\ a \end{array} \right\} = \cos(\theta_L^e - \theta_L^{\nu}) \pm \cos(\theta_R^e - \theta_R^{\nu}) \quad (3.19)$$

so that, to a very good approximation in the limit of small angles, $v \simeq 2$ and $a \simeq 0$.

Clearly, only if $m_E < M_{N,N'}$ will mixing be important in the decays of the E lepton since, in this case E will be stable in the limit of zero mixing. In this case ($M_E < M_{N,N'}$) the decays of the E are quite similar to those of the D quark discussed above except, of course, for the decay $D \rightarrow d + g$. One can then read off the corre-

sponding formulas for the E from the above discussion. For example, in the limit $M_E^2 \ll M_W^2$ (with $M_E < M_{N,N'}$) Table V shows a list of the various branching ratios for E decay. Taking $\Gamma_0 = G_F^2 M_E^5 / 192\pi^3$ we find the total E lifetime to be

$$\Gamma = [9\Delta_L^2 + 14.6(s_R^e c_R^e)^2] \Gamma_0.$$

Note the dependence on both s_R^e and $\Delta_L \equiv \sin(\theta_L^e - \theta_L^{\nu})$ in this case (unlike that for D decay) and the dependence on the ratio $r = (s_R^e c_R^e / \Delta_L)^2$ within the expressions for the branching ratios.

Several points are now in order about two special decay modes: $D \rightarrow d\bar{d}d$ and $E \rightarrow e\bar{e}e$. In calculating these decay rates we have divided by the statistical factor of 2 but we have not included the crossed (t -channel) diagram clearly seen in Fig. 7 for the E decay. These needed to be included in a full-scale calculation of D and E lifetime and branching ratios. Also, in a complete calculation, we need to consider the influence of flavor mixing via the KM matrix—something ignored in our analysis above. We also need to examine the particles in the second and third

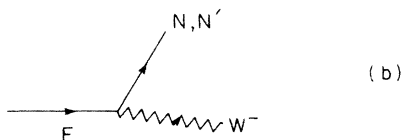
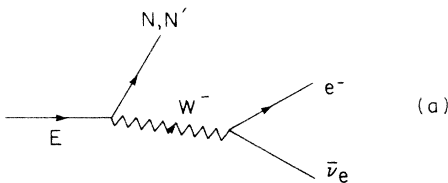


FIG. 6. Diagrams for E -lepton decay via virtual or real W bosons.

TABLE V. Branching ratios of the E in the limit $m_E \gg m_W$.

Mode	Branching ratio
$\nu_e e^- \bar{\nu}_e, \nu_e \mu^- \bar{\nu}_\mu, \nu_e \tau^- \bar{\nu}_\tau$	$(9 + 14.5r)^{-1}$
$\nu_e \bar{u}d, \nu_e \bar{c}s$	$(3 + 4.9r)^{-1}$
$e^- e^+ e^-$	$(35.4r^{-1} + 47.5)^{-1}$
$e^- \mu^+ \mu^-, e^- \tau^+ \tau^-$	$(17.8r^{-1} + 28.8)^{-1}$
$e^- \nu_e \bar{\nu}_e, e^- \nu_\mu \bar{\nu}_\mu, e^- \nu_\tau \bar{\nu}_\tau$	$(9r^{-1} + 14.6)^{-1}$
$e^- u\bar{u}, e^- c\bar{c}$	$(5.0r^{-1} + 8.2)^{-1}$
$e^- d\bar{d}, e^- s\bar{s}, e^- b\bar{b}$	$(4.0r^{-1} + 6.5)^{-1}$

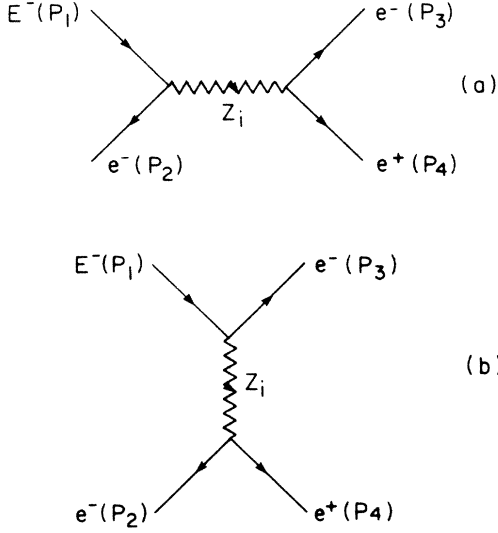


FIG. 7. s - and t -channel diagrams for E -lepton decay into the $e^-e^+e^-$ final state.

generations which correspond to the D and E . The decay modes of these particles can be obtained quite trivially by simple substitution in the above expressions and including appropriate mixing factors.

Our last point concerns our assumption about the mixing between the neutral fermion fields ν_L , ν_R , N_L , N_R , and ν'_L . In our analysis we have made the simplifying assumption that only the pairs of states (ν_L, N_L) and (ν_R, N_R) mix with ν'_L left unmixed. This, effectively, treats the neutral fermions in an identical fashion to the charged fermions as much as possible. In a general theory, however, Majorana mass terms can appear in the natural fermion-mass matrix so that, in principle, mixing can occur between all five of these states leading to a 5×5 mass matrix for each generation of fermions. Clearly, this situation is quite complex (and beyond the scope of this paper) and may lead to some interesting new phenomenology. A full discussion of the decay modes of these neutral fermions must include an analysis of this problem but we will merely continue to use the simplified mixing scenario above for the purposes of our calculations.

IV. PRODUCTION MECHANISMS

For exotic-fermion masses $< M_1$ the most important mechanism for production will be in Z_1 decay. For $2m_f < M_1$, exotic fermions can be pair produced with a decay width given by [assuming a coupling $\bar{f}\gamma_\mu(v - a\gamma_5)fZ_1^\mu$]

$$\Gamma(Z_1 \rightarrow f\bar{f}) = \frac{M_1}{12\pi} \left[1 - \frac{4m_f^2}{M_1^2} \right]^{1/2} \times [v^2(1 + 2m_f^2/M_1^2) + a^2(1 - 4m_f^2/M_1^2)] \quad (4.1)$$

which applies for all fermions but Majorana neutrinos. In that case we obtain a similar result but with $v=0$ and $a^2 \rightarrow 2a^2$. The values of v and a for the new particles can easily be read off from the Lagrangian in Eq. (2.6) and Table II. Note that in the limit of zero mixing $a(D)=a(E)=0$, i.e., both particles couple in a purely vector manner to Z_1 . This is also true for N if it is a Dirac field, whereas only purely axial-vector couplings occur if N_L and N_R are distinct Majorana field. In the crude limit of zero-mass exotics we obtain

$$\frac{\Gamma(Z_1 \rightarrow \bar{E}E)}{\Gamma(Z_1 \rightarrow e^+e^-)} \simeq 1.26, \quad \frac{\Gamma(Z_1 \rightarrow \bar{D}D)}{\Gamma(Z_1 \rightarrow e^+e^-)} \simeq 0.33, \quad (4.2)$$

$$\frac{\Gamma(Z_1 \rightarrow \bar{N}N)}{\Gamma(Z_1 \rightarrow e^+e^-)} \simeq 3.94$$

so that these new fermions would make a substantial change in the overall width of the Z_1 by $\simeq 50\%$ in the zero-mass limit. For $M_D \simeq M_E \simeq 30$ GeV the above values would only be reduced by $\simeq 8\%$ whereas the reduction in the $N\bar{N}$ case would be dependent on whether N was a Dirac field. For N being Dirac the reduction would remain at $\simeq 8\%$ but for $M_{N_L} \simeq M_{N_R} \simeq 30$ GeV we would have a reduction by 55% in the $Z_1 \rightarrow$ exotic neutral fermions yielding only a 30% increase in the Z_1 total width. Clearly for heavier mass values the width is increased by a smaller amount. Present measurements of the width of the Z_1^0 may still be consistent with pair production of exotic fermions as a final state. Since we are assuming that these particles are all light (≤ 46 GeV or so) we are certainly dealing with scenario I of Eq. (3.1) in this case and the exotic fermion will decay via a three-body process. A large fraction of the time these events will materialize as jets-plus-lepton pairs. The nonobservation of such events may indicate exotic masses in excess of $\simeq 40$ GeV.

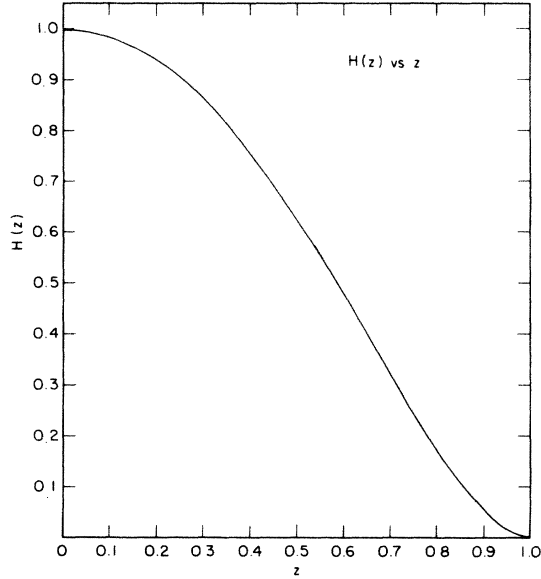
If the exotic particle mass exceeds $\simeq 45$ GeV, then pair production is kinematically forbidden. However, because of mixing, single-particle production is still possible in Z_1 decay with final state such as $e^\pm E^\mp$, $D\bar{d} + D\bar{d}$, $N\bar{\nu} + \bar{N}\nu$, etc., as well as W decay with final states such as $E^- \bar{\nu}_e$ and $D\bar{u}$. (States such as $E^- N$ may also be possible, even in the limit of zero mixing if N is sufficiently light.) If we take the coupling of the exotic-nonexotic pair ($\bar{F}f$) to the gauge boson X to be

$$\bar{F}\gamma_\mu(v - a\gamma_5)fX^\mu + \text{H.c.},$$

then we find (neglecting the mass of f) the decay width to be

$$\Gamma(X \rightarrow \bar{F}f) = \frac{M_X}{12\pi} (v^2 + a^2) (1 - M_F^2/M_X^2)^2 \times (1 + \frac{1}{2}M_F^2/M_X^2). \quad (4.3)$$

For Z_1 decay modes we can read v and a off of Table II and multiply (4.3) by a factor of 2 to include both $\bar{F}\bar{f} + \bar{F}f$ combinations. For W decay, we can obtain v and a directly from Eq. (2.8). Taking $z = M_F/M_X$ and defining the phase-space suppression factor

FIG. 8. H as a function of z defined by Eq. (4.3).

$$H(z) = (1 - z^2)^2 (1 + 1/2z^2)$$

we obtain Fig. 8 showing the amount of phase-space reduction for this process as M_F/M_X increases. Apart from phase-space considerations we find for Z_1 decay the ratios

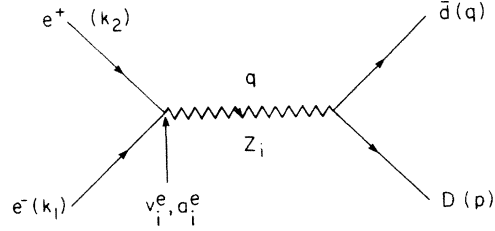
$$\begin{aligned} \frac{\Gamma(Z_1 \rightarrow \bar{E}e + E\bar{e})}{\Gamma(Z_1 \rightarrow e^+e^-)} &= 3.94(s_R^e c_R^e)^2, \\ \frac{\Gamma(Z_1 \rightarrow \bar{D}d + D\bar{d})}{\Gamma(Z_1 \rightarrow e^+e^-)} &= 11.82(s_L^d c_L^d)^2, \\ \frac{\Gamma(Z_1 \rightarrow \bar{N}\nu + N\bar{\nu})}{\Gamma(Z_1 \rightarrow e^+e^-)} &= 3.94(s_R^\nu c_R^\nu)^2, \end{aligned} \quad (4.4)$$

and similarly for W decay modes

$$\begin{aligned} \frac{\Gamma(W^- \rightarrow D\bar{u})}{\Gamma(W^- \rightarrow e^- \bar{\nu}_e)} &= 3(s_L^d)^2, \\ \frac{\Gamma(W^- \rightarrow E^- \bar{\nu}_e)}{\Gamma(W^- \rightarrow e^- \bar{\nu}_e)} &= \sin^2(\theta_L^e - \theta_L^\nu) = \frac{\Gamma(W^- \rightarrow e^- \bar{N})}{\Gamma(W^- \rightarrow e^- \bar{\nu}_e)}. \end{aligned} \quad (4.5)$$

We have assumed that N is a Dirac field in these calculations. If the mixing angles are not too small and the phase-space reduction is not overly drastic these decay modes should be observable. In all cases, since $m_{E,D,N} < M_{W,Z}$ we expect the exotic particles to undergo the usual three-body weak decay and produce observable final-state products. Single-particle production should not make drastic modifications in the Z_1 or W widths due to mixing angle as well as phase-space suppressions although 10% changes are possible. It is quite possible to use present data to get limits on the exotic particle masses but they will be mixing-angle dependent.

If exotic fermions are sufficiently light, one may be able to produce them singly in e^+e^- at center-of-mass ener-

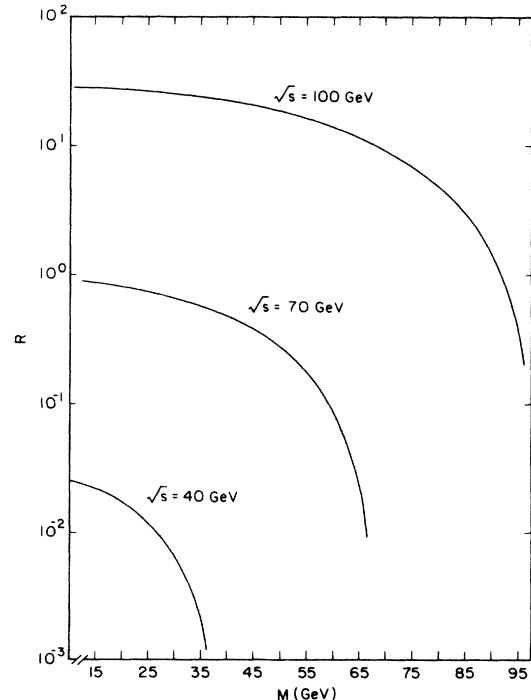
FIG. 9. Diagram responsible for $e^+e^- \rightarrow D\bar{d}$ via virtual $Z_{1,2}$ gauge bosons.

gies below M_1 at, for example, TRISTAN. (The prospects of pair production of exotics below M_1 seem rather remote.) The Feynman diagram for a process such as this is shown in Fig. 9 for the $e^+e^- \rightarrow D\bar{d}$ reaction. The matrix element is given by

$$\begin{aligned} M &= \sum_i \bar{v}(k_2) \gamma_\mu (v_i^e - a_i^e \gamma_5) u(k_1) \bar{u}(p) \gamma^\mu \\ &\quad \times (v_i - a_i \gamma_5) v(q) [(s - M_i^2) - i\Gamma_i M_i]^{-1}, \end{aligned} \quad (4.6)$$

where the sum extends over the gauge boson $Z_{1,2}$. The generic differential cross section obtained in this manner is given by ($z = \cos\theta$)

$$\begin{aligned} \frac{d\sigma(e^+e^- \rightarrow F\bar{f})}{dz} &= \sum_{ij} \frac{N_c s}{32\pi} (1 - M^2/s) [1 - (M^2/s)^2] \\ &\quad \times A_{ij} [B_{ij}(1 + \beta z^2) + C_{ij}(1 + \beta)z], \end{aligned} \quad (4.7)$$

FIG. 10. Cross section for single-exotic-fermion production in e^+e^- collisions scaled to $\sigma(e^+e^- \rightarrow \mu^+\mu^-)$ via a single Z^0 . The curves shown need to be rescaled by a factor of $(s_R^e c_R^e)^2$.

where $\beta \equiv (s - M^2)/(s + M^2)$, N_c is the number of colors of $F\bar{f}$, and

$$\begin{aligned} B_{ij} &\equiv (v_i v_j + a_i a_j)(v_i^e v_j^e + a_i^e a_j^e), \\ C_{ij} &\equiv (v_i a_j + a_i v_j)(v_i^e a_j^e + a_i^e v_j^e), \end{aligned} \quad (4.8)$$

with A_{ij} given by Eq. (3.6) with the replacement $q^2 \rightarrow s$. Note θ is defined as the angle between the e^- and the F . For $e^+e^- \rightarrow \bar{F}f$ we obtain the same result with $z \rightarrow -z$ keeping the same definition of the angle. Upon integration over z , the odd term vanishes and $1 + \beta z^2 \rightarrow 2(3 + \beta)/3$ yielding the total cross section.

As an example, we have calculated the total cross section for $e^+e^- \rightarrow \mu^+M^- + \mu^-M^+$ where M is the muon's exotic partner in this limit $M_2 \rightarrow \infty$. The result is shown in Fig. 10 where we have plotted the ratio

$$R \equiv \frac{\sigma(e^+e^- \rightarrow \mu^+M^- + \mu^-M^+)}{\sigma(e^+e^- \rightarrow \mu^+\mu^-)} \quad (4.9)$$

as a function of the exotic-fermion mass for three different center-of-mass energies. This process then takes place via the usual Z^0 and the FCNC $\bar{\mu}M$ coupling. Therefore, our results need to be multiplied by $(s_K^{\mu} c_K^{\mu})^2$ which may provide a significant reduction in total cross section. Similar results are obtainable for $\bar{D}d + D\bar{d}$ production, etc., but special care needs to be taken in the case of $\bar{E}e + E\bar{e}$ production due to the existence of the t -

$$\begin{aligned} \frac{d\sigma}{dx dy} &= \sum_q \sum_{ij} \frac{s}{8\pi} x A_{ij} \{ [(1 - \lambda/x) + (1 - y - \lambda/x)][q(x) + \bar{q}(x)] \alpha_{ij} \\ &\quad + [(1 - \lambda/x) - (1 - y)(1 - y - \lambda/x)][q(x) - \bar{q}(x)] \beta_{ij} \}, \end{aligned} \quad (4.10)$$

where $q(x)$ [$\bar{q}(x)$] is the relevant quark [antiquark] distribution function (which is also Q^2 dependent), and x and y are the usual scaling variables with

$$\begin{aligned} \lambda &\leq x \leq 1, \\ 0 &\leq y \leq 1 - \lambda/x, \end{aligned} \quad (4.11)$$

and

$$\begin{aligned} \alpha_{ij} &= (v_i v_j + a_i a_j)(v_i^e v_j^e + a_i^e a_j^e), \\ \beta_{ij} &= (v_i a_j + v_j a_i)(v_i^e a_j^e + v_j^e a_i^e). \end{aligned} \quad (4.12)$$

It may be possible to produce E -type leptons with masses of order 100 GeV by this mechanism but detailed calculations of the cross section (4.10) are hampered by the unknown values of the mixing angles and the mass of the Z_2 .

V. HIGGS-BOSON PHYSICS

As has been noted earlier,⁷ the simple Higgs sector of the SM needs to be extended in order to give mass to all the fermions and the additional $U(1)_X$ gauge bosons. The simplest toy model of this kind simply adds a complex isosinglet field ϕ'_0 to the usual isodoublet field Φ . In any realistic model, however, additional isodoublets and isosinglets with differing $U(1)_X$ quantum numbers need to be

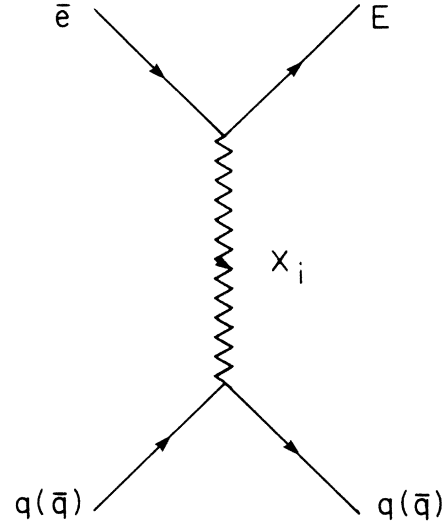


FIG. 11. Single- E -lepton production in ep collision.

channel graph as shown in Fig. 7 for E decay.

E -type leptons can also be produced in high-energy ep colliders such as DESY HERA with $\sqrt{s} = 314$ GeV. The diagram for this process is shown in Fig. 11. With $\lambda = M^2/s$ the differential cross section for single E production ($ep \rightarrow E + X$) is given by

added. To investigate some of the new physics associated with the extended Higgs sectors in such theories it is sufficient, however, to consider the toy model outlined above. Denoting

$$\Phi = \begin{bmatrix} \phi^+ \\ \phi^0 \end{bmatrix}, \quad \phi' = (\phi'_0), \quad (5.1)$$

the scalar potential takes the form

$$\begin{aligned} V &= -\mu_2^2 \Phi^\dagger \Phi + \lambda_2 (\Phi^\dagger \Phi)^2 - \mu_1^2 (\phi'^\dagger \phi') \\ &\quad + \lambda_1 (\phi'^\dagger \phi')^2 + \kappa (\Phi^\dagger \Phi) (\phi'^\dagger \phi'). \end{aligned} \quad (5.2)$$

The neutral fields are then shifted [we ignore the possibilities of complex vacuum expectation values (VEV's)]

$$\phi^0 = \frac{\chi_2 + i\eta_2 + v_2}{\sqrt{2}}, \quad \phi'_0 = \frac{\chi_1 + i\eta_1 + v_1}{\sqrt{2}}. \quad (5.3)$$

Then $\eta_{1,2}$ become the would-be Goldstone bosons which together with ϕ^\pm are "eaten" by the W^\pm and $Z_{1,2}$ gauge bosons to produce their longitudinal components. The $\chi_{1,2}$ fields remain as physical states with a mass-squared matrix of the form

$$M^2 = \begin{bmatrix} 2\lambda_1 v_1^2 & \kappa v_1 v_2 \\ \kappa v_1 v_2 & 2\lambda_2 v_2^2 \end{bmatrix} \quad (5.4)$$

which, of course, reduces to the usual results in the $\kappa \rightarrow 0$ limit. M^2 is diagonalizable by a suitable rotation by an angle

$$\tan 2\phi = \frac{\kappa v_1 v_2}{|\lambda_2 v_2^2 - \lambda_1 v_1^2|} \quad (5.5)$$

such that the physical neutral Higgs fields are given by

$$\begin{aligned} H_1^0 &= \chi_1 \cos\phi + \chi_2 \sin\phi, \\ H_2^0 &= \chi_2 \cos\phi - \chi_1 \sin\phi \end{aligned} \quad (5.6)$$

with mass eigenvalues

$$M_{1,2}^2 = (\lambda_1 v_1 + \lambda_2 v_2) \pm [(\lambda_1 v_1 - \lambda_2 v_2)^2 + 4\kappa^2 v_1 v_2]^{1/2}. \quad (5.7)$$

As an application of this let us consider the general form of the charged lepton and $Q = -\frac{1}{3}$ quark-mass matrices for a single generation. For leptons, the general fermion-Higgs-boson coupling takes the form

$$\begin{aligned} L_{eH} &= \frac{c_1}{\sqrt{2}} \bar{e}_L^0 e_R^0 (\chi_2 + v_2) + \frac{c_4}{\sqrt{2}} \bar{E}_L^0 E_R^0 (\chi_1 + v_1) \\ &+ \frac{c_3}{\sqrt{2}} \bar{e}_L^0 E_R^0 (\chi_1 + v_1) \\ &+ \frac{c_2}{\sqrt{2}} \bar{E}_L^0 e_R^0 (\chi_2 + v_2) + \text{H.c.}, \end{aligned} \quad (5.8)$$

where the c_i are numerical coefficients some of which may be zero. e^0 , E^0 , etc. denotes the weak-eigenstate basis. Equation (5.8) can be rewritten as

$$L_{eH} = \bar{\mathcal{E}}_L^0 M \mathcal{E}_R^0 + \text{H.c.} \quad (5.9)$$

using the notation of Eq. (2.3) with

$$M = \frac{1}{\sqrt{2}} \begin{bmatrix} c_1 v_2 & c_3 v_1 \\ c_2 v_2 & c_4 v_1 \end{bmatrix}. \quad (5.10)$$

M_e is then diagonalizable by a bi-unitary transformation since

$$\mathcal{E}_{L,R} = U_{L,R} \mathcal{E}_{L,R}^0 \quad (5.11)$$

$$L_{FC} = \frac{1}{\sqrt{2}} (\bar{e}_L E_R + \bar{E}_R e_L) \{ [c_1 (s_L^e c_R^e - c_L^e s_R^e) + (c_L^e c_R^e + s_L^e s_R^e)] \chi_2 + [c_3 (c_L^e c_R^e + s_L^e s_R^e) + c_4 (c_L s_R - s_L c_R)] \chi_1 \}. \quad (5.17)$$

$\chi_{1,2}$ then need to be rotated into the physical field $H_{1,2}^0$ via Eq. (5.6). Thus we find

$$L_{FC} = \bar{e} (\alpha_i - \beta_i \gamma_i) E (\kappa_1 H_1^0 + \kappa_2 H_2^0) + \text{H.c.}, \quad (5.18)$$

where κ_i can be read off from (5.17) and (5.6). Coupling such as (5.20) may have many phenomenological implications such as modifying the $g-2$ of the electron and muon by a substantial amount. We find¹³ (with m_i the mass of H_i)

$$\Delta a_e = \frac{m_e^2}{8\pi^2} \sum_i k_i^2 \int_0^1 dx \frac{x^2 - x^3 + (m_E/m_e)x^2}{m_e^2 x^2 + (m_E^2 - m_e^2)x + m_i^2(1-x)} (\alpha_i^2 - \beta_i^2) \quad (5.19)$$

which in the limit $m_e/m_E \rightarrow 0$ and $x_i = m_i^2/M_E^2$ becomes

$$\begin{aligned} \Delta a_e &= \frac{1}{8\pi^2} \frac{m_e}{M_E} \sum_i k_i^2 (1-x_i^2)^{-3} (\frac{1}{2} - 2x_i + \frac{2}{3}x_i^2 - x_i^2 \ln x_i) (\alpha_i^2 - \beta_i^2) \\ &\equiv \frac{1}{8\pi^2} \frac{m_e}{M_E} \sum_i k_i^2 F(x_i) (\alpha_i^2 - \beta_i^2). \end{aligned} \quad (5.20)$$

and

$$U_L^\dagger M U_R = M_{\text{diag}} \quad (5.12)$$

with M_{diag} being the diagonalized mass matrix. To obtain U_L (U_R) we form the combination MM^\dagger ($M^\dagger M$) which is Hermitian and diagonalizable in the usual way to M_{diag}^2 by U_L (U_R). MM^\dagger and $M_e^\dagger M$ are explicitly

$$MM^\dagger = \frac{1}{2} \begin{bmatrix} c_1^2 v_2^2 + c_3^2 v_1^2 & c_1 c_2 v_2^2 + c_3 c_4 v_1^2 \\ c_1 c_2 v_2^2 + c_3 c_4 v_1^2 & c_2^2 v_2^2 + c_4^2 v_1^2 \end{bmatrix}, \quad (5.13)$$

$$M^\dagger M = \frac{1}{2} \begin{bmatrix} (c_1^2 c_2^2) v_2^2 & (c_1 c_3 + c_2 c_4) v_1 v_2 \\ (c_1 c_3 + c_2 c_4) v_1 v_2 & (c_3^2 + c_4^2) v_1^2 \end{bmatrix},$$

and have quite different dependence on the VEV's. Note that if all c_i were equal θ_L^e (the angle in U_L) would be 45° whereas

$$\tan 2\theta_R^e = \frac{2v_1 v_2}{v_1^2 - v_2^2} \quad (5.14)$$

which is VEV dependent. Also note in the $v_2/v_1 \rightarrow 0$ limit, $\theta_R^e \rightarrow 0$ whereas θ_L^e remains 45° . It should be remembered from our phenomenological discussions above that θ_R^e must be small whereas only the difference $\theta_L^e - \theta_R^e$ must be small.

A similar situation occurs for the $Q = -\frac{1}{3}$ charged quarks. Here

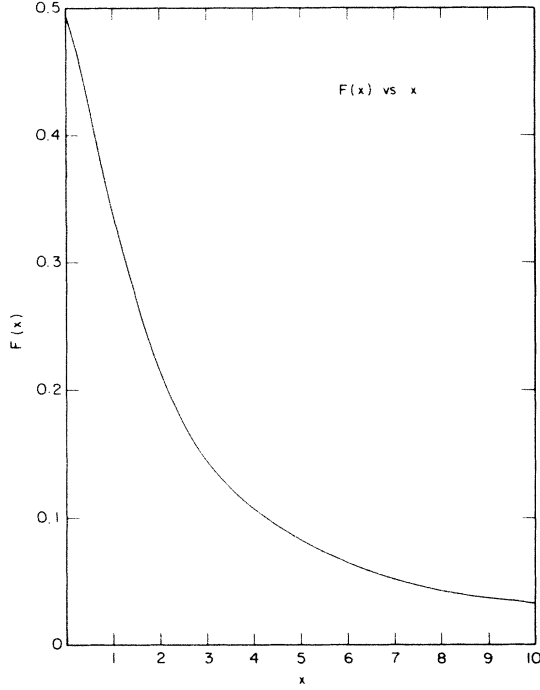
$$L_{dH} = \bar{\mathcal{D}}_L^0 M \mathcal{D}_k^0 + \text{H.c.}, \quad (5.15)$$

with

$$M = \frac{1}{\sqrt{2}} \begin{bmatrix} a_1 v_2 & a_3 v_2 \\ a_2 v_1 & a_4 v_1 \end{bmatrix}. \quad (5.16)$$

Note $M(d)$ resembles $M^\dagger(e)$ and *not* $M(e)$. This implies that for a_i all equal we obtain $\theta_R^d = 45^\circ$ while θ_L^d is given by (5.14). Note that it is θ_L^d which is constrained to be small by phenomenology.

The mixing of the (e^0, E^0) fields produce a neutral-Higgs-boson coupling which is flavor changing of the form

FIG. 12. F as a function of x defined in Eq. (5.22).

The function $F(x)$ is shown in Fig. 12 and varies between 0 and $\frac{1}{2}$ as x is varied from 0 to ∞ . To show that Δa_e is large let us take $m_1 = m_2$, $k_1 = k_2 = k$, etc., such that ($x_i \simeq 1.5$ being a typical value)

$$\sum_i k_i^2 F(x_i) (\alpha_i^2 - \beta_i^2) = \frac{1}{2} k^2 (\alpha^2 - \beta^2). \quad (5.21)$$

Now with $m_E \simeq 100$ GeV we obtain the result

$$\Delta a_e \simeq 3 \times 10^{-8} k^2 (\alpha^2 - \beta^2). \quad (5.22)$$

Clearly $k^2 (\alpha^2 - \beta^2) \leq 10^{-3} - 10^{-4}$ in order not to violate the good agreement between QED and the experiment. A similar result is obtained for the muon

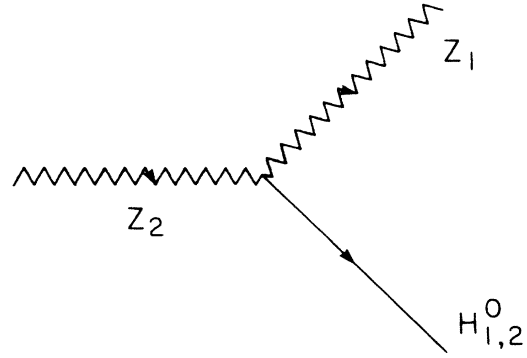
$$\Delta a_\mu \simeq 7 \times 10^{-6} k^2 (\alpha^2 - \beta^2)$$

implying that $k^2 (\alpha^2 - \beta^2)$ is again $\lesssim 10^{-3} - 10^{-4}$. Obviously one can use the constraints from the $g-2$ of the electron and muon to constrain the Higgs sector parameters and various mixing angles as well. A more complete analysis, however, needs to be done and the effects of vector particle exchange included.⁷

As a last consequence of Higgs-boson physics we consider the decay $Z_2 \rightarrow Z_1 + H_i^0$ (as shown in Fig. 13) which may compete with ordinary fermion-antifermion pairs as a Z_2 decay mode. The $Z_2 Z_1 H_i$ coupling arises from the Φ -field covariant derivative; we find a coupling

$$2 \frac{gg_X}{c_W} v_2 t_3 t_X Z_\mu^2 Z^\mu (H_2^0 \cos \phi + H_1^0 \sin \phi), \quad (5.23)$$

where t_3 and t_X are the eigenvalues of the generators T_3 and T_X for the neutral number of the Φ field. (Clearly ϕ' cannot induce this coupling because $T_3 \phi' = 0$.) Thus with $t_3 = -\frac{1}{2}$ and t_X left arbitrary we find

FIG. 13. Diagram for $Z_2 \rightarrow Z_1 + H_{1,2}^0$.

$$\begin{aligned} \Gamma(Z_2 \rightarrow Z_1 + H_i^0) &= \frac{M_2}{48\pi} \frac{a^2}{M_2^2} \left[\left(1 + \frac{m_1^2 - m_H^2}{m_2^2} \right)^2 - 4 \frac{m_1^2}{m_2^2} \right]^{1/2} \\ &\times \left\{ 2 + \left[\left(1 + \frac{m_1^2 - m_H^2}{m_2^2} \right) / (2m_1/m_2) \right]^2 \right\} \left\{ \frac{c_\phi^2}{s_\phi^2} \right\}, \end{aligned} \quad (5.24)$$

where

$$a^2 = \left[\frac{gg_X}{c_W} v_2 t_X \right]^2 = 4g_X^4 M_1^2 t_X. \quad (5.25)$$

Neglecting phase-space suppression this yields

$$\Gamma(Z_2 \rightarrow Z_1 + H_i) = \frac{M_2}{12\pi} g_X^2 \left[g_X^2 \frac{M_1^2}{M_2^2} \right] \left\{ \frac{c_\phi^2}{s_\phi^2} \right\} \quad (5.26)$$

compared with the fermion-antifermion decay rate

$$\Gamma(Z_2 \rightarrow \bar{f}f) = \frac{M_2}{12\pi} g_X^2 (v_X^2 + a_X^2). \quad (5.27)$$

Clearly, even with phase-space suppression from finite Z_1 and H mass effects the $Z_1 H$ final state may be $\simeq 10\%$ of a typical $\bar{f}f$ mode. This may have important consequences for probing Higgs-boson physics once the Z_2 is discovered.

VI. CONCLUSION

In this paper we have begun to examine the new low-energy phenomenology associated with the breaking of E_6 GUT's resulting from superstrings. We have concentrated on the properties of the new particles as well as the extension of the electroweak sector by an additional $U(1)$ factor expected in all such theories.

The decay properties of the new exotic fermions are quite distinctive and differ substantially from a fourth sequential generation of fermions. This difference arises mainly from the decays which follow from the existence

of flavor-changing neutral currents and the small mixing between the ordinary and exotic fermions. Very unusual final states are found to be possible such as SUSY particles, gauge bosons, and gluons.

Various production mechanisms were examined for these new particles; these analyses indicate that these new particles should be observed at existing accelerators or those under construction if they are sufficiently light and mixing angles are not too small.

The mass matrices of these new fermions were examined as were some implication of an extended Higgs sector such as the modification of the value of $g - 2$ for the electron and muon and a new decay mode of the new neutral gauge boson Z_2 .

We are just beginning to examine the phenomenology resulting from superstring theories and exploring the implications of E_6 is the first step.

After this work was completed, we received a paper from Barger, Deshpande, Phillips, and Whisnant,¹⁴ who also considered the phenomenology of exotic fermions in E_6 theories.

ACKNOWLEDGMENT

This work was supported by the U.S. Department of Energy, Contract No. W-7405-Eng-82, Office of Energy Research (KA-01-01), Division of High Energy and Nuclear Physics.

¹J. H. Schwarz, Phys. Rep. **89**, 223 (1982); G. T. Horowitz, UCSB report, 1985 (unpublished); C. B. Thorn, in *Unified String Theories*, proceedings of the Workshop, Santa Barbara, 1985, edited by M. B. Green and D. J. Gross (World Scientific, Singapore, 1985).

²For a recent work on E_6 not directly related to superstrings see, for example, R. W. Robinett and J. L. Rosner, Phys. Rev. D **26**, 2356 (1982); R. W. Robinett, *ibid.* **26**, 2388 (1982); P. K. Mohapatra, R. N. Mohapatra, and P. B. Pal, University of Maryland report 1985 (unpublished); P. H. Frampton and T. W. Kephart, Phys. Rev. D **25**, 1459 (1982); A. Sen, Phys. Rev. Lett. **55**, 33 (1985).

³M. B. Green and J. H. Schwarz, Phys. Lett. **149B**, 117 (1984); P. Candelas, G. T. Horowitz, A. Strominger, and E. Witten, Nucl. Phys. **B258**, 46 (1985); E. Witten, Phys. Lett. **149B**, 351 (1984); D. J. Gross, J. Harvey, E. Martinec, and R. Rohm, Phys. Rev. Lett. **54**, 46 (1985); Nucl. Phys. **B256**, 253 (1985).

⁴E. W. Kolb, D. Seckel, and M. S. Turner, Fermilab Report No. CONF-85 1114A, 1985 (unpublished); Fermilab Report No. Pub-85-016-A, 1985 (unpublished).

⁵For some recent work on mirror fermions see, for example, J. Ollivier and C. Albright, Phys. Lett. **160B**, 121 (1985); S. Mishra, S. P. Misra, S. Panda, and U. Sarkar, University of Calcutta Report No. IP/BBSR/84-12 (unpublished); G. Senjanović, F. Wilczek, and A. Zee, Phys. Lett. **141B**, 389 (1984); J. Maalampi and M. Ross, *ibid.* **146B**, 333 (1984); S. Rajpoot and J. G. Taylor, *ibid.* **142B**, 365 (1984); D. Forigon and M. Roos, *ibid.* **147B**, 34 (1984); M. Roos, *ibid.* **135B**, 487 (1984).

⁶B. A. Ovrut, University of Pennsylvania report, 1985 (unpublished); S. Cecotti, J.-P. Derendinger, S. Ferrar, and L. Girardello, Phys. Lett. **156B**, 318 (1985); S. M. Barr, Phys. Rev. Lett. **55**, 2278 (1985); R. Holman and D. Reiss, Fermilab Report No. Pub-85/130-A (unpublished); M. Dine, Institute for Advanced Studies report, 1985 (unpublished); M. Dine, V. Koplunovsky, M. Mangano, C. Nappi, and N. Seiberg, Nucl. Phys. B (to be published); E. Witten, *ibid.* Nucl. Phys. **B258**,

75 (1985); Y. Hosotani, Phys. Lett. **126B**, 309 (1983); J. P. Derendinger, L. E. Ibanez, and H. P. Nilles, CERN Report No. CERN-TH-4228/85 (unpublished); J. Rosner, Enrico Fermi Institute Report No. EFIL85-34, 1985 (unpublished); V. Barger, N. G. Deshpande, and K. Whisnant, Phys. Rev. Lett. **56**, 30 (1986); V. Barger, N. Deshpande, R. J. N. Phillips, and K. Whisnant, Phys. Rev. D **33**, 1912 (1986); P. Kalyniak and M. K. Sundaresan, Carleton University report, 1985 (unpublished); L. E. Ibanez, CERN Report No. CERN-TH.4308/85, 1985 (unpublished); M. Drees, N. K. Falck, and M. Glück, University of Dortmund Report No. DO-TH 85/25, 1985 (unpublished); L. S. Durkin and P. Langacker, Phys. Lett. **166B**, 436 (1985); E. Cohen, J. Ellis, K. Enquist, and D. V. Nanopoulos, Phys. Lett. **166B**, 436 (1985); Phys. Lett. **161B**, 85 (1985); CERN Report No. TH-4222, 1985 (unpublished).

⁷J. L. Hewett, T. G. Rizzo, and J. A. Robinson, Phys. Rev. D (to be published).

⁸R. W. Robinett, Phys. Rev. D **33**, 1408 (1986); T. G. Rizzo, *ibid.* **33**, 3329 (1986); Report No. IS-J 2040, 1985 (unpublished); J. L. Rosner, Enrico Fermi Institute Report No. EFI-85-34, 1985 (unpublished).

⁹S. L. Glashow and S. Weinberg, Phys. Rev. D **15**, 1958 (1971); E. A. Pachos, *ibid.* **15**, 1966 (1977).

¹⁰T. G. Rizzo, Phys. Rev. D **33**, 3329 (1986); Report No. IS-J 2037, 1986 (unpublished).

¹¹M. Kobayashi and T. Maskawa, Prog. Theor. Phys. **40**, 652 (1973).

¹²For a general review of the constraints implied by cosmology see K. A. Olive, talk given at the Twelfth Texas Symposium on Relativistic Astrophysics, Jerusalem, 1984 (unpublished), and references therein.

¹³See, for example, J. Leveille, Nucl. Phys. **B137**, G3 (1977).

¹⁴V. Barger, N. Deshpande, R. J. N. Phillips, and K. Whisnant, Phys. Rev. D **33**, 1912 (1986).